Photografted Poly(ethylene glycol) Matrix for Affinity Interaction Studies

Andréas Larsson, Tobias Ekblad, Olof Andersson, and Bo Liedberg*

Division of Sensor Science and Molecular Physics, Department of Physics, Chemistry and Biology, Linköping University, SE-581 83 Linköping, Sweden

Received July 14, 2006; Revised Manuscript Received September 20, 2006

A poly(ethylene glycol) (PEG)-based matrix for studies of affinity interactions is developed and demonstrated. The PEG matrix, less than 0.1 μm thick, is graft copolymerized onto a cycloolefin polymer from a mixture of PEG methacrylates using a free radical reaction initiated by UV light at 254 nm. The grafting process is monitored in real time, and characteristics such as thickness, homogeneity, relative composition, photostability, and performance in terms of protein resistance in complex biofluids and sensor qualities are investigated with null ellipsometry, infrared spectroscopy, and surface plasmon resonance. The matrix is subsequently modified to contain carboxyl groups, thereby making it possible to immobilize ligands in a controlled and functional manner. Human serum albumin and fibrinogen are immobilized and successfully detected by antibody recognition using surface plasmon resonance. The results are encouraging and suggest that the PEG matrix is suitable for biochip and biosensor applications in demanding biofluids.

Introduction

In biosensor applications it is highly interesting to employ surface-enlarging matrixes (hydrogels) which combine the property of low nonspecific binding with the ability to immobilize ligands, ranging from small molecules to proteins and ultimately to cells. Possibly the most commonly used one is the carboxymethylated (CM) dextran matrix.[1] However, this type of matrix is not always the ideal choice, since nonspecific binding is frequently encountered in work involving complex biological solutions such as serum, plasma, and cell lysates. Problems with nonspecific binding in CM dextran have been reported when heparin binding is investigated such as the complement components factor B and factor P[2,3] and in interaction studies between high-motility-group proteins and DNA.[4] Alternative matrixes are therefore of interest. Poly(ethylene glycol) (PEG) in different forms has proven to be a suitable material for construction of protein-resistant surfaces for biomaterial applications.[5−9] For that reason, PEG is a promising candidate when a biosensor matrix is being designed. Previous studies on non-cross-linked PEG-based matrixes describe coatings of cationic poly(L-lysine)-functionalized PEG on metal oxide surfaces[10−12] and grafting of PEG molecules under low pressure and elevated temperature onto water plasma activated silicon.[13] Another attractive route is to produce PEG matrixes by free radical grafting of PEG-containing acrylate or methacrylate monomers. Such reactions can be initiated chemically[14] or thermally[15] or by electromagnetic radiation. A less commonly used but very attractive method relies on electrografting.[16] During photoinduced grafting, the radiation is often in the UV range, and various substrates, such as polymers,[5,17−22] thiols on gold,[23] and silanes on silicon/silicon dioxide,[24] have been explored. However, none of these studies were aimed at biosensing. Reports on PEG-based biosensor systems involve heat-induced grafting of PEG chains on silanized silicon surfaces,[25] cationic poly(L-lysine)-functionalized PEG deposited onto niobium oxide substrates,[26] and disulfide PEG molecules adsorbed onto gold.[2,27] In these cases, the PEG chains had a second functionality, *N*-hydroxysuccinimide (NHS), biotin, carboxyl, and amine groups, respectively.

In the present study, a PEG matrix for biosensor applications is produced by a UV-initiated free radical polymerization at 254 nm. A hydroxyl-terminated PEG methacrylate monomer, with an average chain length of 10 ethylene glycol units (PEG_{10}-MA), is graft copolymerized with another, less complicated, methacrylate monomer, 2-hydroxyethyl methacrylate (HEMA), onto an air plasma treated cycloolefin polymer (COP)-coated substrate. The underlying substrate is oxidized silicon or gold depending on the mode of examination. During the air plasma treatment, the polymer surface is oxidized and groups such as hydroxyl, ether, peroxide, carbonyl, and carboxyl are introduced on the surface.[28] In particular, the formed peroxides are considered to be a prerequisite for efficient grafting.[29,30] When UV-initiated radical grafting is used, the sample is commonly placed in a UV-transparent glass container containing the aqueous monomer solution. The thicknesses of films produced this way have been reported to fall in the range from nanometers[24] to micrometers[18] depending on the reaction conditions. Here we employ a less commonly used sandwich approach where an aqueous solution containing the monomers (240 mM) is confined between the COP-coated substrate and a quartz disk. A similar methodology based on grafting from a neat monomer solution was recently reported by Wang et al.[22] The proposed process is illustrated in Figure 1. This route of production leads to a thin matrix (<0.1 μm) containing a high density of terminal hydroxyl groups, which can be used for further modification, thereby vouching for an efficient sensor. After the copolymerization reaction, the matrix is successfully modified to express carboxyl groups using a modification chemistry described elsewhere.[1] Subsequently, the carboxyl groups are activated using *N*-ethyl-*N'*-[3-(dimethylamino)propyl]carbodiimide (EDC)/NHS, a method commonly used to immobilize proteins via lysine residues.

The grafting process is monitored with null ellipsometry (NE) and infrared (IR) spectroscopy in the dry state and in situ with

* To whom correspondence should be addressed. E-mail: bolie@ifm.liu.se.

10.1021/bm060685g CCC: \$37.00
Published on Web 11/21/2006

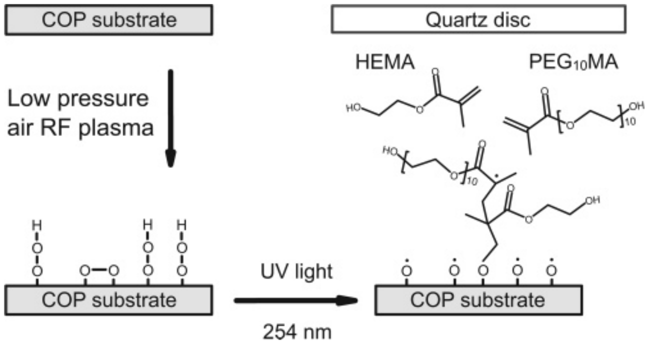

Figure 1. Proposed process of producing the PEG matrix. Peroxides and other reactive species are induced on the COP surface upon air plasma treatment. UV irradiation generates surface radicals, which interact with monomers ($PEG_{10}MA$ and HEMA) in the solution. A grafting chain reaction is thereby initiated, and a matrix is formed.

surface plasmon resonance (SPR), and much emphasis is devoted to studies aiming at improving the understanding of the matrix formation process and relative composition. The protein-rejecting properties of the unmodified matrix, after exposure to a single-component protein solution of human fibrinogen (Fib) as well as to complex biological biofluids such as serum and plasma, are evaluated with NE. Moreover, IR reflection−absorption spectroscopy is used to follow the entire process from an unmodified matrix, through a carboxylation and activation/immobilization/deactivation sequence, to interaction between the immobilized protein and a corresponding polyclonal antibody. Finally, the performance of the matrix in a series of antigen/antibody experiments is demonstrated using SPR.

Taken together, we have developed a PEG-based matrix, <0.1 μm thick, which displays excellent protein-rejecting properties. Furthermore, the possibility to immobilize ligands and study the interaction with analytes makes this matrix a very promising alternative for studies of affinity interactions in real time using technologies based on label-free optical or gravimetric detection schemes.

Materials and Methods

Reagents. $PEG_{10}MA$, HEMA, bromoacetic acid, *N*-hydroxysuccinimide, ethanolamine, and human serum albumin (HSA) were purchased from Sigma-Aldrich Sweden AB. *N*-Ethyl-*N′*-[3-(dimethylamino)-propyl]carbodiimide was obtained from Biacore AB, Uppsala, Sweden. Human fibrinogen was purchased from Hyphen BioMed SAS, France. Polyclonal rabbit anti-HSA (aHSA) and polyclonal rabbit anti-human fibrinogen (aFib) were obtained from DakoCytomation Denmark A/S, and rabbit anti-egg white lysozyme (aLys) was obtained from Rockland Immunochemicals. Sodium hydroxide was purchased from Merck KGaA, Germany. The cycloolefin polymer Zeonor 1020R was obtained as a generous gift from Åmic AB, Uppsala, Sweden.

Substrate Preparation. Silicon (100) wafers (Siltronic AG, Germany) with a native oxide layer were coated with gold and used as substrates for IR experiments. First, the wafers were cut into 20 × 40 mm pieces, cleaned in a 6:1:1 mixture of Milli-Q water (Milli-Q, Millipore), 30% hydrogen peroxide (Merck KGaA), and 37% hydrogen chloride (Merck KGaA) for 10 min at 85 °C (TL-2 procedure), and thoroughly rinsed in Milli-Q water. The surfaces were then dried with nitrogen gas in a laminar flow bench prior to being coated with 25 Å of titanium (Balzers, Liechtenstein, 99.9%) and 2000 Å of gold (Nordic High Vacuum AB, Kullavik, Sweden, 99.99%) by electron beam evaporation. The equipment used was a Balzers UMS 500 P system. The evaporation rate was 1 and 10 Å/s for titanium and gold, respectively. The base pressure was at least 10^{-9} mbar, and the pressure during evaporation was on the low 10^{-7} mbar scale. Silicon substrates of 12.5 × 12.5 mm size were used without metal coating for ellipsometric measurements. Gold-coated (thickness of 440 Å) 12 × 12 mm glass substrates for SPR experiments were obtained as a generous gift from Biacore AB.

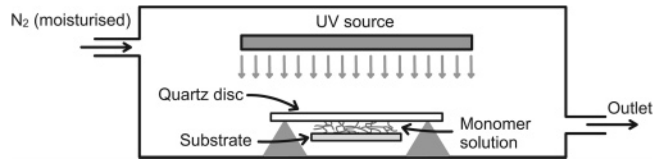

Figure 2. Schematic illustration of the reaction chamber, provided with a 254 nm light source, and the free-hanging sample substrate.

COP-Based Grafting and Matrix Carboxylation. PEG matrixes were prepared in the same manner on both oxidized silicon and gold substrates. After an initial 5 min ultrasonication in ethanol, 99.5% (Kemetyl AB, Sweden), the surfaces were radio frequency plasma treated for 1 min at 200 W in air at a pressure below 0.01 mbar (Pico, Diener Electronic GmbH, Germany). This plasma treatment was used to ensure secure adhesion of the subsequently deposited COP film. To minimize the presence of dust, the surfaces were then rinsed in ethanol and dried with nitrogen gas in a laminar flow bench. A COP film of about 85 Å was then spin coated onto the surfaces (0.25%, w/v, COP in xylene (Sigma-Aldrich Sweden AB); step 1, speed 2000 rpm, acceleration 664 rpm/s^2, 30 s; step 2, speed 3000 rpm, acceleration 1245 rpm/s^2, 5 s) using a WS-400B-6NPP/Lite spin coater (Laurell Technologies Corp.). To create active groups on the COP surfaces, they were air plasma treated for 6 s at 160 W (pressure below 0.01 mbar). In the process, the thickness of the COP film was decreased to approximately 60 Å.

After substrate activation, an amount of monomer solution depending on the substrate size (0.05 μL/mm^2) was placed on the underside of a UV-transparent quartz disk, previously cleaned in a 5:1:1 mixture of Milli-Q water, 30% hydrogen peroxide, and 25% ammonia (Merck KGaA) for 10 min at 85 °C (TL-1 procedure). The quartz disk and the COP substrate were then brought together to form a sandwich assembly, in which the sample COP substrate became *free-hanging* below the quartz disk, and kept in place by the surface tension of the liquid. The thickness of the monomer solution was estimated to be 30 ± 10 μm. The sandwich assembly was then inserted into the reaction chamber and placed on supports (Figure 2). The reaction chamber, which was constructed in-house, was purged with nitrogen for 1 min before and during 0−14 min of exposure to UV light. To prevent the solvent from evaporating, the nitrogen gas was moisturized with Milli-Q water before entering the chamber. The light source had a distinct emission peak at 254 nm (Philips TUV PL-L 18 W), and the distance between the quartz disk and the lamp was 30 mm. Different mixtures of $PEG_{10}MA$ and HEMA in Milli-Q water were investigated at a total monomer concentration of 240 mM. After grafting, the samples were ultrasonicated for 5 min in ethanol and dried in nitrogen gas. To obtain terminal carboxyl groups in the matrix, the samples were incubated in an aqueous solution of 1 M bromoacetic acid and 2 M sodium hydroxide for 16 h at room temperature during shaking.[1] This reaction transforms −*O*H groups into −*O*CH_2COOH groups. Samples that were not examined immediately were stored under nitrogen.

Null Ellipsometry. The instrument used for ellipsometric measurements was an automatic Rudolph Research AutoEL ellipsometer equipped with a He−Ne laser (λ = 632.8 nm) set at an angle of incidence of 70°. Each sample surface was measured at five spots. The refractive index used for the COP, the PEG matrix, and immobilized molecules in the dry state was 1.5. A series of samples where the ratio between the monomers varied ($PEG_{10}MA$:HEMA = 0:1, 9:1, 3:1, 1:1, 1:3, 1:9, and 1:0), but the time of irradiation was kept constant at 8 min, was prepared and examined with NE. In addition, a time series where a 1:1 composition was irradiated for 0, 1, 2, 4, 6, 8, 10, 12, and 14 min was studied. Moreover, the degrading nature of the UV radiation was evaluated after matrixes of three compositions (0:1, 1:1, and 1:0, prepared using 8 min of UV exposure) were irradiated for 2, 4, 8, and 14 min in the absence of monomer solution. The samples used for nonspecific protein adsorption experiments were prepared from a 1:1 mixture using 8 min of UV exposure.

Infrared Spectroscopy. A Bruker IFS 66 system, equipped with a liquid nitrogen cooled mercury cadmium telluride (MCT) detector, was utilized to record the reflection−absorption (RA) spectra. The incident light was aligned at a grazing angle of 85°. To minimize the presence of water in the measurement chamber, it was purged with nitrogen gas. The resolution was 2 cm^{-1}, and a three-term Blackman Harris apodization function was applied to the interferograms prior to Fourier transformation. A deuterated hexadecanethiol ($HS(CD_2)_{15}CD_3$) self-assembled monolayer on gold was used to record the background spectra. All IR experiments were performed on gold substrates. A series of samples where the ratio between the monomers varied (0:1, 9:1, 3:1, 1:1, 1:3, 1:9, and 1:0), but the time of irradiation was kept constant at 8 min, was studied with IR. Degradation experiments on pure PEG_{10}-MA and HEMA matrixes, respectively, were undertaken by recording the infrared RA spectrum before and after 14 min of UV exposure in the absence of monomers. Protein immobilization and interaction experiments were carried out on 1:1 mixture samples, irradiated with UV for 8 min. Prior to protein immobilization, the carboxylated matrix was activated for 30 min with an aqueous mixture of EDC and NHS at 0.2 and 0.05 M,[1] respectively. HSA (700 nM) in 10 mM sodium acetate buffer, pH 4.5, was then immobilized for 60 min. Subsequently, the matrix was deactivated with an aqueous solution of 1 M ethanolamine[1] for 30 min, to remove remaining succinimide groups in the matrix, and finally incubated in 300 nM aHSA in HBS−EP buffer (10 mM Hepes, 0.15 M NaCl, 3 mM EDTA, 0.005% polysorbate 20, pH 7.4) for 60 min.

Surface Plasmon Resonance. SPR measurements during grafting were carried out using an in-house custom-built instrument. The SPR instrument consisted of two rotation stages with synchronously movable arms. Surface plasmons were excited by means of a prism, on top of which the grafting sandwich assembly (substrate, monomer solution, and quartz disk) was placed. P-polarized, monochromatic (760 nm interference filter) light from a fixed collimated source was guided toward the prism using mirrors mounted on one of the movable arms. A CCD detector with imaging optics was mounted onto the other arm. A refractive index matching gel was used to achieve optical contact between the substrate and the prism. The UV light source was placed at a distance of 30 mm above the quartz disk, and a 1:1 monomer solution was used. During grafting, the setup was purged with moisturized nitrogen gas. SPR curves were sampled nearly every 30 s.

The SPR experiments to study the functionality were undertaken on a BiacoreX instrument equipped with two temperature-controlled flow channels, which were kept at 25.0 °C. The flow rate was 5 μL/min, and the running buffer was HBS−EP. All PEG matrixes used in these SPR experiments were obtained from a 1:1 mixture that had been irradiated with UV light for 8 min. After carboxylation, the terminal carboxyl groups in the matrix were activated by a 5 min injection of an aqueous mixture of EDC and NHS at 0.2 and 0.05 M,[1] respectively. After immobilization of the ligand, an aqueous solution of 1 M ethanolamine[1] with a contact time of 7 min was used to deactivate the matrix. To demonstrate the sensor qualities of the PEG matrix, HSA at a concentration of 700 nM in 10 mM sodium acetate buffer, pH 4.5, was injected during the immobilization step with a contact time of 5 min. After deactivation, the matrix was exposed to 7 min of 300 nM aFib as a negative control. Finally, 300 nM aHSA was injected for 7 min. Both antibodies were diluted in HBS−EP buffer. An identical experiment in terms of concentrations and contact times was performed, where Fib was immobilized and exposed to aLys and aFib.

Results and Discussion

Hydrogel Preparation and Characterization. The uniformity and the reproducibility of the matrix thickness are critical issues to address when matrixes for biosensor applications are being developed. Four parameters were found to have great impact on the above characteristics, namely, the total concentration of monomer(s), their relative composition, the volume of the monomer solution and thereby the thickness of the liquid film formed between the substrate and the quartz disk, and finally the time of exposure to UV radiation. Considerable efforts were made to optimize these parameters. Two of them remained constant throughout this work, namely, the volume of the monomer solution, which was kept at 0.05 $\mu L/mm^2$, and the total monomer concentration, 240 mM. The ellipsometric thicknesses of matrixes generated from different mixing ratios of the two monomers PEG_{10}MA and HEMA are shown in Figure 3. The uniformity and reproducibility are generally very good in cases when PEG_{10}MA is the dominating monomer in the solution, although the resulting matrixes become slightly thinner when the PEG_{10}MA content increases above 50%. However, the process is clearly negatively affected and less controlled when the HEMA content is increased above 50%. The variation in thickness within a sample as well as between a set of samples prepared from the same mixture increases with the HEMA content, and this is particularly evident for the 1:9 and 0:1 compositions, Figure 3. The matrix reaches a maximum thickness of ∼900 Å at a solution composition of 9:1 before it returns back to ∼400 Å for pure HEMA matrixes. A more detailed discussion on the origin of this behavior follows in subsequent sections. Taken together, monomer mixtures with PEG_{10}MA as the main component seem to give reproducible matrixes of superior quality, and it was decided to stick to matrixes prepared from 1:1 mixtures in the studies on nonspecific adsorption and functionality.

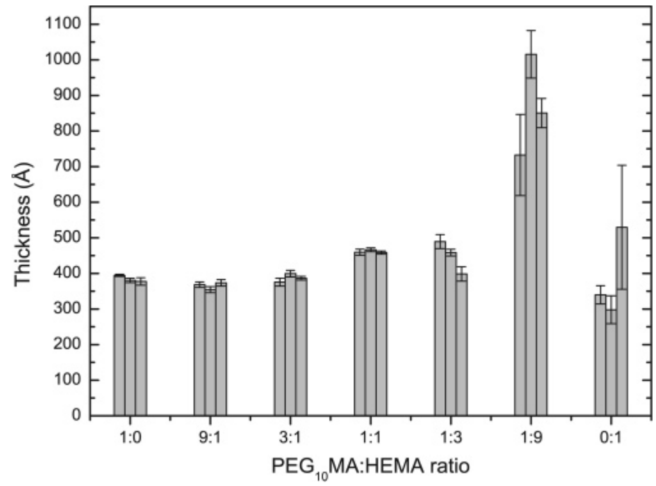

Figure 3. Ellipsometric thickness of matrixes on COP-coated silicon, grafted in an aqueous solution containing various mixtures of PEG_{10}-MA and HEMA. Three samples were examined at each concentration, and the UV exposure time was 8 min in all cases. The error bars represent the standard deviation from five measurements on each sample.

Furthermore, IR spectroscopy is used to study the structure and composition of the matrix. Figure 4 displays the infrared RA spectra of the different monomer compositions in the CH and fingerprint regions, respectively, and as can be seen they share many common features. The following peak assignments are given for the 1:1 composition. The ester carbonyl C=O, adjacent to the polymer backbone, is clearly seen at 1732 cm^{-1}. For better comparison the spectra were normalized with respect to the intensity of this peak, since each monomer (building block) contains one carbonyl group only. This normalization procedure enables us to compare matrixes of varying thickness

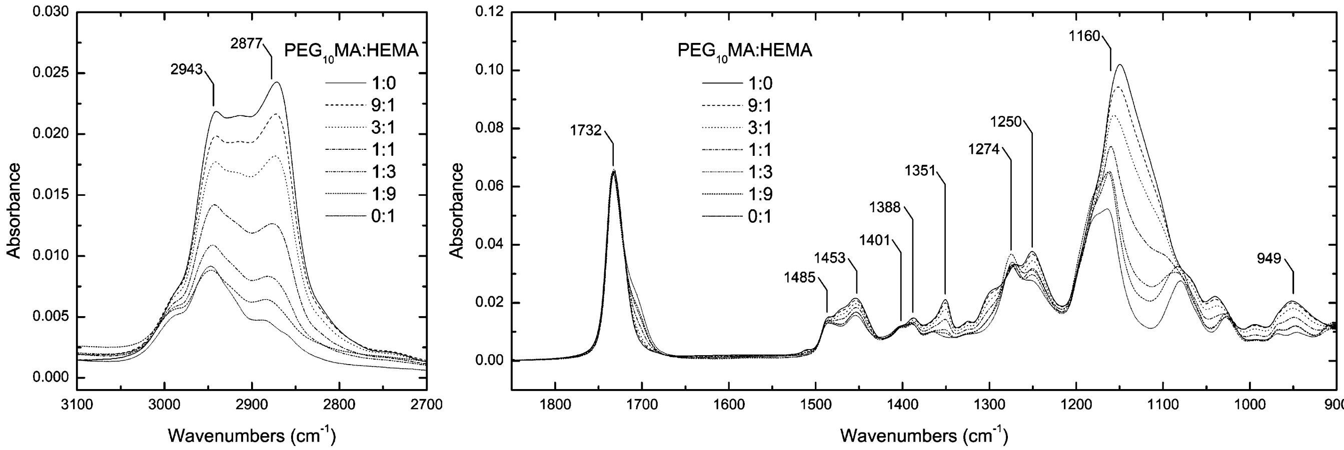

Figure 4. Infrared RA spectra of matrixes prepared on COP-coated gold from different mixtures of $PEG_{10}MA$ and HEMA. The peak positions in the spectra are those assigned to the 1:1 composition. All data have been normalized with respect to the intensity of the peak at 1732 cm^{-1}, corresponding to the C═O vibration of the backbone of the matrix.

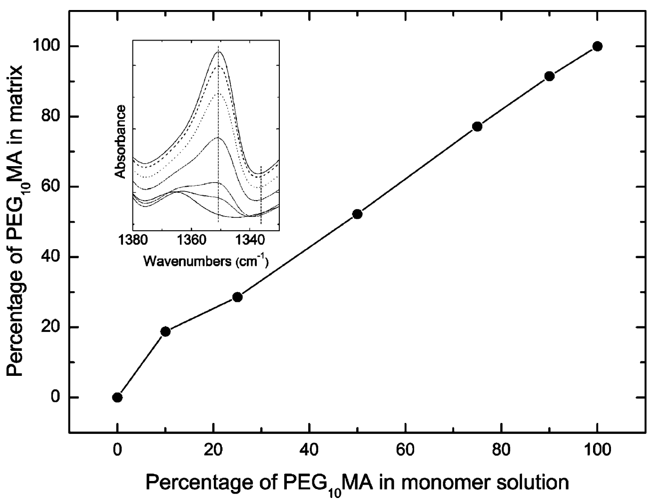

Figure 5. Relation between monomer composition in the solution and in the generated matrix. The data are based on integration of the peak at 1351 cm^{-1} in the RA spectra, Figure 4. Inset: Blowup around the 1351 cm^{-1} peak, Figure 4. The integration limits (1351 and 1336 cm^{-1}) are shown as vertical dashed lines.

having the same number of building blocks. Asymmetric CH_2 stretches appear at 2943 cm^{-1} and symmetric CH_2 stretches at 2877 cm^{-1}. The CH_2 scissoring modes are observed at 1485 and 1453 cm^{-1}, while peaks at 1401, 1388, and 1351 cm^{-1} are assigned to CH_2 wagging modes. Twisting modes of CH_2 appear at 1274 and 1250 cm^{-1}, and rocking modes are found at 949 cm^{-1}. The C−O−C stretches in the PEG chain are found at 1160 and ∼1100 cm^{-1}.

To elucidate the relation between monomer composition in the solution and in the generated matrix, the peak at 1351 cm^{-1} has been integrated between 1351 and 1336 cm^{-1}, normalized to the integrated intensity obtained for the pure $PEG_{10}MA$ matrix, and finally plotted versus the solution composition, Figure 5. It is seen that the relation between the matrix and solution composition is nearly linear. Note again that the behavior of the 1:9 (10%) composition deviates from the overall trend, in line with the ellipsometric data in Figure 3. The origin of this deviation is not fully clear, but it might be related to the photoinstability of HEMA; see below.

Growth and Degradation of the Matrix. A series of matrixes generated from a 1:1 mixture were subjected to UV light for different periods of time, 0−14 min, to reveal the thickness dependence on UV exposure time. Ellipsometric data from these experiments are given in Figure 6A. The thickness

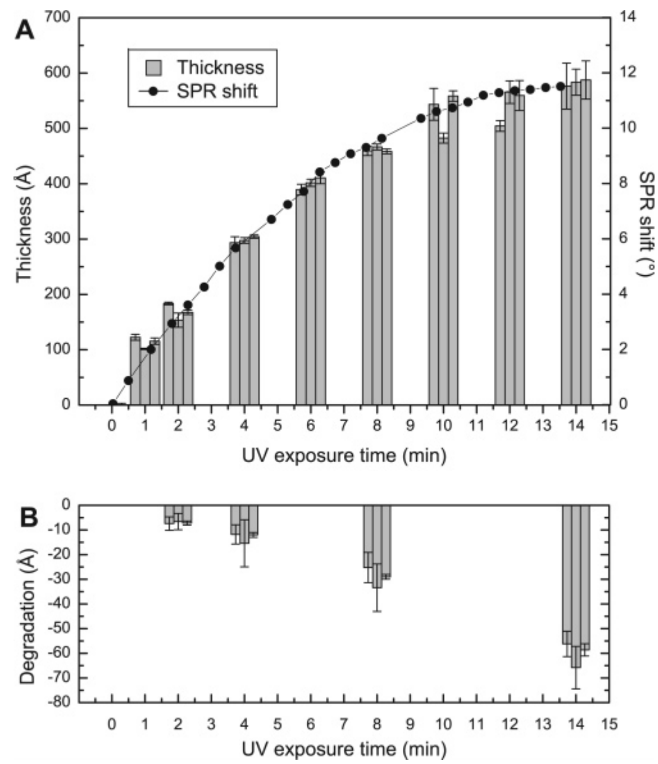

Figure 6. (A) Ellipsometric data showing the growth of 1:1 matrixes on COP-coated silicon. Three samples were examined at each of the time points 0, 1, 2, 4, 6, 8, 10, 12, and 14 min. The error bars represent the standard deviation from five measurements on each sample. Filled circles describe the shift in SPR angle measured in real time during the grafting process on gold. (B) Ellipsometric experiments showing the degradation of 1:1 matrixes on silicon. Three samples were examined at each degradation time. The error bars represent the standard deviation from five measurements on each sample.

levels off at ∼600 Å after 12 min, and the variation in thickness, both within a particular sample and between a set of identically prepared samples, is generally very small. The growth was also monitored in real time using SPR. The shifts in SPR angle during the grafting process (filled circles) show excellent agreement with the ellipsometric data (bars) (Figure 6A). From these measurements it is evident that the growth rate decreases with time. In a related study on spontaneous grafting of a PEG_6-MA monomer (containing six ethylene glycol units) at room temperature onto α-bromoester-functionalized silicon, Xu et al.[14] reported a growth curve with the same general appearance as the one in Figure 6A. However, to achieve a thickness of 600 Å, an exposure time of 3−4 h was needed. Nho et al.[31] grafted HEMA and PEG$_x$MA (various $x < 10$) onto cellulose substrates using elevated temperatures, and they also reported a decreasing polymerization rate with increasing reaction time. No ellipsometric thicknesses were given in that work, but the reactions were allowed to proceed for up to 4 h. One explanation to the decreasing polymerization rate could be that the concentration of monomers in the solution becomes too low to allow for efficient grafting. Thus, our findings as well as those of Nho[31] suggest that the grafting efficiency per molecule decreases with decreasing monomer concentration (a constant grafting efficiency per molecule would correspond to a linear curve). In other words, the lower the monomer concentration, the lower the grafting rate. One way to avoid this behavior, and thereby obtain thicker matrixes, could be to continuously supply the reaction chamber with a constant concentration of monomers via a fluidic system.

It should be noted, however, that UV irradiation contributes not only to the growth of the matrix, but also to the degradation of it. In the present work, NE experiments, where the 1:1 matrix has been subjected to UV light in the absence of monomers (but otherwise under the same conditions as previously) after the initial grafting process, show that the matrix decreases in thickness with increasing UV exposure time (Figure 6B). As can be seen, the degree of degradation is almost linearly dependent on exposure time to UV light. Hence, the overall growth of the matrix seems to be limited by (i) monomer depletion during grafting and (ii) UV degradation, the latter of which which appears to occur at a constant rate. To elucidate the UV sensitivity of the two components, degradation experiments were also performed on pure PEG$_{10}$MA and HEMA matrixes. The thickness and spectral appearance were measured after 0−14 min of UV irradiation, and the results from ellipsometric and IR experiments are depicted in parts A and B, respectively, of Figure 7. Both techniques undoubtedly reveal that pure HEMA matrixes are very sensitive to UV light, while pure PEG$_{10}$MA matrixes seem to be resistant. The mechanism(s) behind the improved photostability of PEG$_{10}$MA is at present not understood. We merely conclude that an extended ethylene glycol substituent has a positive effect on the overall photostability of PEG$_{10}$MA-based matrixes. This observation may explain the somewhat puzzling data found in Figure 3, where the grafting is more efficient and the thickness increases with increasing content of HEMA (cf. the 9:1 mixture in Figure 3), except in the case when pure HEMA is used. In the latter case, there are no PEG chains present, leaving the backbone unprotected and vulnerable to UV degradation. In other words, the apparent higher reactivity of HEMA is counteracted by its sensitivity to UV light.

Nonspecific Adsorption. The protein-rejecting properties of PEGs are well documented,[5−9] and the underlying reasons are normally ascribed to its waterlike character and high motility as well as the fact that it is noncharged. The similarity to water results in minimal interfacial energy at the PEG/water interface. Therefore, proteins approaching such an interface will not be greatly affected. The high motility of the PEG chains in water has been explained by the favorable way in which they coordinate the water molecules and thereby obtain liquidlike flexibility. A concept often discussed in this context is steric stabilization, which has two contributions, namely, a volume restriction term and an osmotic term. Volume restriction describes the reduction in the number of available conformations of the PEG chains upon interaction with an approaching protein.

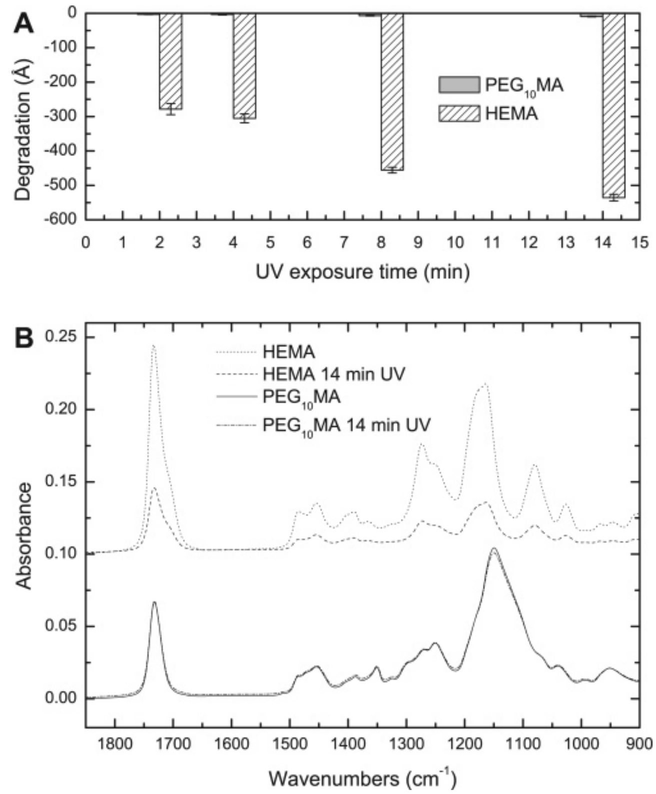

Figure 7. Degradation of single-component matrixes upon UV irradiation in the absence of methacrylate monomers. (A) Ellipsometric experiments on pure PEG$_{10}$MA and HEMA matrixes on COP-coated gold substrates. One sample of each was examined after 2, 4, 8, and 14 min. The error bars represent the standard deviation from five measurements on each sample. (B) Infrared RA spectra before and after 14 min of UV exposure. The upper two curves have been offset for clarity.

As a result, the conformational entropy is lowered and adsorption is counteracted. The osmotic term is associated with a local increase in PEG concentration upon compression by approaching proteins. An osmotic force develops as the distance between PEG chains is shortened, whereby the chains are repelled, which in effect reduces protein adsorption.[32,33] The absence of hydrogen bond donors is also reported to correlate to protein resistance.[34]

In a recent study Unsworth et al.[35] utilized single protein solutions of Fib to deduce how the length and density of self-assembled PEG chains affected the protein adsorption. The molecular masses of the used chains were between 750 and 5000 Da, and the density was varied by using different incubation conditions. An optimum in the Fib resistance was found at intermediate chain densities for all tested chain lengths, indicating that the chain density is a critical parameter. Apart from longer PEG chains, shorter oligo(ethylene glycol) (OEG) (∼2−8 EG units) chains have been used with success to prevent nonspecific protein adsorption. It seems that at least two to three EG units are necessary to obtain satisfactory protein resistance. When this small number of EG units is used, the terminal group plays an important role and a hydroxyl group is preferred, whereas for six EG units and above, a terminal methoxy group also may be used.[36−38]

The nonspecific protein adsorption of the present 1:1 matrix was investigated at 22 °C using ellipsometric measurements before and after incubation of the matrixes in 0.4 mg/mL Fib, 80% heparinized human plasma, and 67% human serum. The incubation time was 30 min, and the buffer used was phosphate-buffered saline (PBS) (10 mM sodium hydrogen phosphate, 10

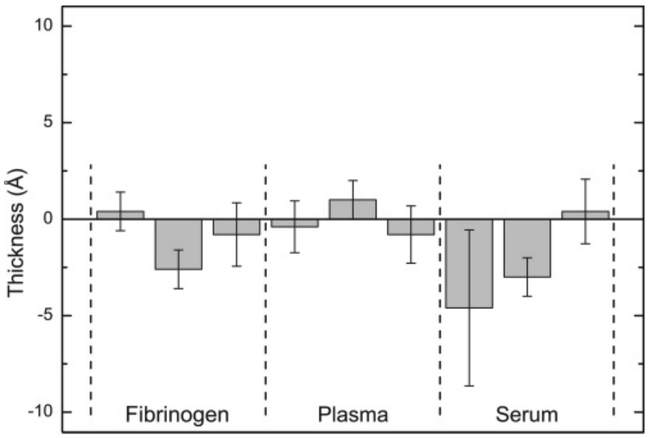

Figure 8. Nonspecific protein adsorption onto the PEG matrix (1:1) prepared on COP-coated silicon and recorded with NE. Three samples were incubated at 22 °C in 0.4 mg/mL Fib, 80% heparinized human plasma, and 67% human serum, respectively. All incubations lasted for 30 min in PBS, pH 7.4. The error bars represent the standard deviation from five measurements on each sample.

mM potassium dihydrogen phosphate, and 150 mM sodium chloride), pH 7.4. Fibrinogen was chosen due to its "sticky" nature, and plasma and serum are complex biological solutions that are known to cause nonspecific adsorption. As can be seen in Figure 8, the PEG matrix possesses outstanding protein-rejecting properties in all cases. The protein adsorption is very low; in fact, it seems to approach the detection limit (~1 Å) of the instrument. Some values are negative, which may be attributed to a slight washing effect of the protein and buffer solutions. However, these changes are below 5 Å, which corresponds to ≤1% of the total thickness of the matrix. To put these values into context, the protein adsorption from 80% heparinized plasma onto an untreated COP film is about 80 Å, while it is on the order of 50 Å from serum and Fib, using the same incubation protocol.

Although much work has been performed on the interactions between PEG surfaces and buffered single protein solutions, not many comprehensive studies have been carried out using blood plasma or serum as the protein solution. Such studies give a more accurate account of the adsorption that might take place upon blood contact, which is often the ultimate application of biomaterials or biosensor surfaces. The available literature shows, in accordance with the current study, that PEG surfaces, under the right circumstances, can maintain low protein adsorption even in contact with blood plasma. For instance, when using a method similar to that in this work, Lee et al. demonstrated a 90% reduction of protein adsorption from 1% plasma on surfaces grafted with $PEG_{10}MA$, compared to unmodified polyethylene.[8] Other studies have investigated surfaces coated with the PEG-containing surfactant Pluronic and found these to reduce protein adsorption from plasma.[39] Some of the most convincing results have been reached with PEG-functionalized poly(L-lysine) surfaces, which almost completely suppress protein adsorption from serum and heparinized plasma.[40,41]

It is clear from the presented results that a random copolymer of $PEG_{10}MA$ and HEMA can meet the necessary requirements for obtaining an inert matrix for label-free biosensing applications. The results are especially interesting since the PEG chains used are relatively short. While most previous studies have focused on longer chains, with molecular masses in the kDa range, the current study demonstrates that, with sufficient surface coverage and chain density, shorter PEG chains can result in very low levels of nonspecific protein adsorption. This approach is successfully applied to prevent nonspecific adsorption in the discussed complex biological solutions at 22 °C, a temperature commonly used in biosensor applications.

Functionality: Matrix Carboxylation, Immobilization, and Specific Interactions. The hydroxyl terminals in the matrix were used to introduce numerous carboxyl groups, schematically outlined in Figure 9, by the method developed by Löfås et al.[1] Other routes are also available, and one example is described in the work done by Wang et al.[22] where a PEG_6MA-based matrix and a carboxylation process involving succinic anhydride and pyridine were used. In the $PEGCOO^-$ spectrum, Figure 10, the presence of the carboxylate groups, close to the backbone (originating from HEMA) and at the terminus of PEG chains (originating from $PEG_{10}MA$), are clearly seen as asymmetric stretches at 1609 and ~1585 cm^{-1}, respectively. These COO^- stretching peaks do not appear unless the sample is treated with an alkaline solution before measurement. A comparison between the infrared RA spectra (data not shown) before and after the fairly harsh carboxylation step[1] reveals no changes except those discussed and seen in Figure 10. Thus, it can be concluded that the present matrix can be successfully carboxylated without having its integrity affected.

The possibility to immobilize proteins in the matrix and subsequently study specific and nonspecific interactions was evaluated using infrared RA spectroscopy and SPR. Besides the RA spectra of unmodified and carboxylated 1:1 matrixes, Figure 10 displays the spectra of the matrix after activation with EDC/NHS, immobilization of HSA, deactivation with ethanolamine, and interaction with aHSA. After activation and immobilization of HSA (HSA spectrum), amide I and II peaks appear at 1660 and 1544 cm^{-1}, respectively. The amide peaks are characteristic for proteins, and it is therefore concluded that the protein was indeed immobilized properly. The excess NHS groups are also detected via the ester carbonyl C═O stretches at 1816 and 1789 cm^{-1}.[42] As expected, deactivation of the matrix with ethanolamine (EtAmine spectrum) leads to a further increase of the amide peaks and a concomitant reduction of the intensity of the NHS peaks. The incubation in aHSA (aHSA spectrum) gives rise to antibody binding due to the specific interaction with HSA and hence to even larger amide peaks. Thus, it has been demonstrated that a protein which has been covalently immobilized in the matrix can be detected using a specific antibody.

Moreover, Figure 11A shows a typical SPR sensorgram of matrix activation, immobilization of HSA, deactivation with EtAmine, nonspecific interaction with aFib, and specific interaction with aHSA. In Figure 11B an SPR sensorgram for a similar experiment is shown, where Fib is immobilized and interacts nonspecifically with aLys and specifically with aFib. It is evident that nonspecific binding is nonexistent, while there is a very clear specific response of the two analytes aHSA and aFib in the respective sensorgrams. One-to-one aHSA occupancy of HSA would correspond to an aHSA response of 10620 RU, whereas the actual response is 2117 RU or approximately 20% of the one-to-one occupancy. The corresponding one-to-one aFib occupancy of Fib would correspond to an aFib response of 3027 RU. In this case the actual response is 2082 RU or approximately 70% of the one-to-one occupancy. At a first glance, the matrix seems to be better suited for large proteins. However, it should be remembered that the antibodies used here are polyclonal, and therefore, it may be possible for the larger protein Fib (M_w = 340 kDa) to bind more than one antibody, whereas the smaller protein HSA (M_w = 66 kDa) is probably sterically hindered to accommodate more than one antibody (M_w = 146 kDa) after being covalently immobilized. This issue

CDV

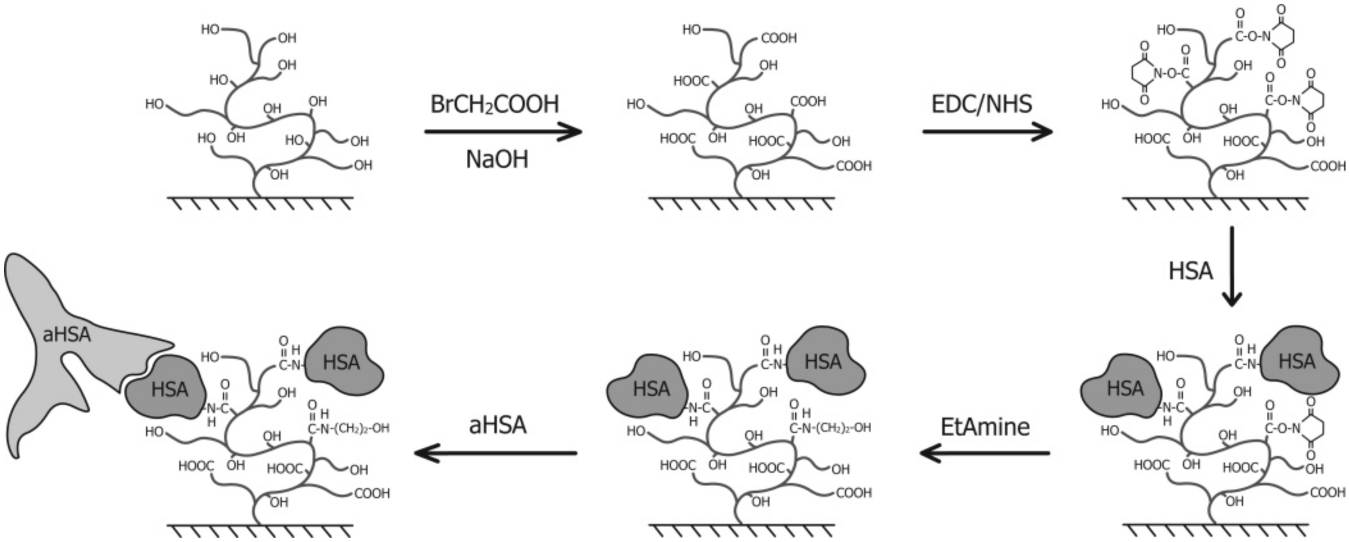

Figure 9. Schematic illustration of the PEG matrix before and after carboxylation, activation, protein immobilization, deactivation, and specific interaction with a corresponding antibody. The overall production process from grafting to immobilization/deactivation takes 18 h, primarily due to a lengthy carboxylation reaction. Note that the $-O$H groups are transformed into $-OCH_2COOH$ groups in the first reaction step and that the linker $-OCH_2-$ has been omitted for clarity.

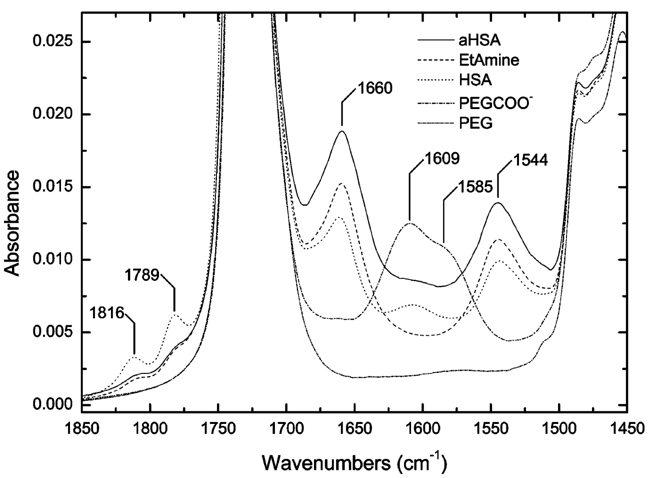

Figure 10. Infrared RA spectra covering the carboxylation and activation/immobilization/deactivation sequence as well as the interaction between the immobilized protein and its corresponding antibody. The sample used was a 1:1 matrix on COP-coated gold. Key: PEG, PEG matrix before carboxylation; PEGCOO$^-$, carboxylated PEG matrix; HSA, EDC/NHS activated and HSA immobilized; EtAmine, deactivated with ethanolamine; aHSA, binding of aHSA.

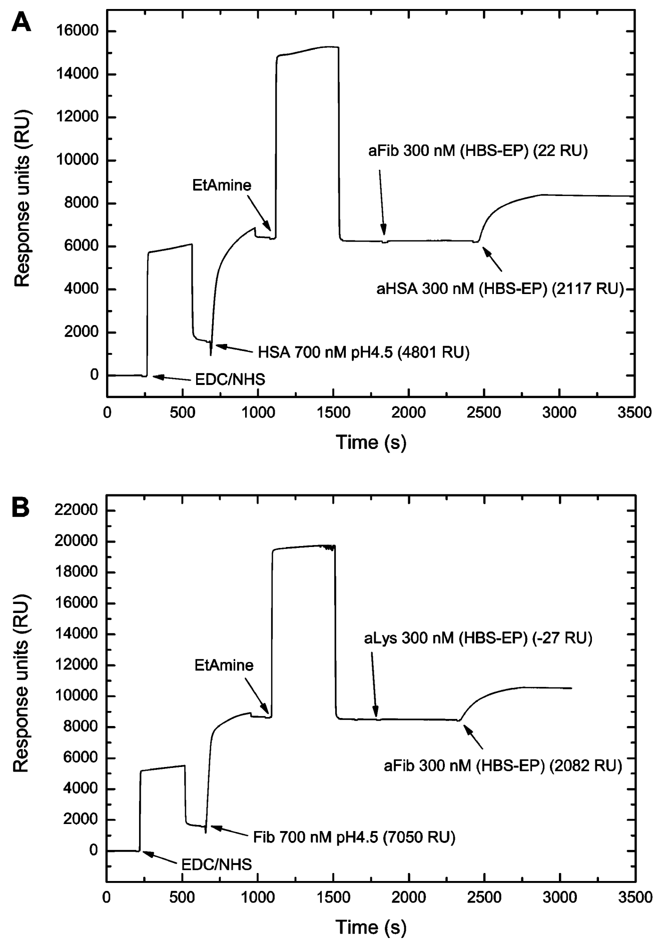

Figure 11. Typical SPR sensorgrams exhibiting different interaction events in carboxylated 1:1 matrixes. After activation with EDC/NHS, the ligands (A, HSA; B, Fib) were immobilized. Thereafter the matrixes were deactivated using ethanolamine. The nonspecific binding was evaluated by an injection of an antibody with specificity to a protein not present (A, aFib; B, aLys). Finally the analytes (A, aHSA; B, aFib) were injected to display the specific interaction.

should be addressed by repeating the experiment with monoclonal antibodies. Furthermore, immobilizations of differently sized proteins indicate that the matrix offers size selectivity where small proteins are favored (to be published elsewhere). In the comparison between the HSA−aHSA and the Fib−aFib interactions, the better performance of the latter can be partly explained by the size selectivity. Due to their mutual size differences, every place in the matrix where Fib can go, aFib can also reach, whereas HSA can go to places that aHSA is excluded from. One of the reasons for the observed size selectivity may be the remarkably high degree of EDC/NHS activation seen as a response of more than 1600 RU in Figure 11. A typical response obtained for a carboxymethylated dextran matrix (CM5) is 100−400 RU.[43] This comparison suggests that a large amount of carboxyl groups can be activated in the PEG matrix, which in turn might lead to multiple attachment points of immobilized proteins. Due to their size, large proteins should be more prone to show this behavior. In effect, the matrix would then become heavily cross-linked, a phenomenon that undoubtedly will influence the penetration of analyte proteins. One way to circumvent this behavior may be to shorten the carboxylation reaction time. An alternative, more elegant solution would be to use precarboxylated monomers in a mixture of hydroxyl-terminated $PEG_{10}MA$ and HEMA. In this way, the content of chemical handles (COOH groups) can be tuned and optimized with ease. In addition, issues regarding possible variations in the activity of the carboxyl groups close to the backbone (originating from HEMA) and at PEG chains (originating from $PEG_{10}MA$) can be addressed separately. Due to the seemingly high content of activated carboxyl groups in the present PEG matrix, it is important to make sure that they are properly deactivated after immobilization of the ligand. Otherwise, at pH values above the isoelectric point of the carboxyl groups, the charges from the caboxylate groups form a negative background that is likely to contribute to nonspecific adsorption of proteins.

Conclusions

A fully functional biosensor matrix composed of a mixture of relatively short ethylene glycol segments (~10) has been generated on COP-coated substrates using UV-initiated radical polymerization of PEG-substituted methacrylates. Detailed infrared and ellipsometric studies reveal the matrixes generated from equimolar mixtures of $PEG_{10}MA$ and HEMA display excellent protein-rejecting properties upon exposure to Fib, serum, and heparinized plasma. Furthermore, the terminal OH groups offer a convenient target for carboxylation and subsequent covalent immobilization of proteins, and the activity of proteins immobilized in that way is probed by SPR using polyclonal antibodies. The overall production process of the biochip is rather time-consuming (18 h), and nearly 90% of the time is devoted to the carboxylation step. No efforts have been made to optimize this step. An alternative route would be to use precarboxylated monomers, thereby making the postcarboxylation procedure redundant. Not only would this speed up the process, it would also provide opportunities to fine-tune the content of carboxyl groups in the matrix by mixing with noncarboxylated and inert methacrylate monomers. Moreover, the large number of commercially available methacrylate monomers with different chain lengths and functional groups enables the production of matrixes optimized for different applications. Small molecule detection, for example, is generally favored by dense and compact matrixes, with a large number of anchoring sites and huge loading capacity, whereas large and complex biomolecules and cells require flexible, hydrogel-like, matrixes. Grafting in other types of solvents could also provide means of affecting the density of the matrix, e.g., for size-selective filtering of biomolecules.

Using COP as the basic platform for the matrix production makes this approach highly versatile since COP can be spin coated onto a wide range of substrates. In addition, it should be noted that this grafting technique can be applied on self-supported sheets of COP. This type of polymer material is easily moulded to form microsized structures, which facilitates fast and cheap production of small-scale sensor systems, possibly with integrated sample preparation and detection on-chip.[44]

Apart from grafting onto a COP polymer, self-assembled monolayers of thiols on gold can be used as grafting platforms. Various terminal groups, such as hydroxyl, carboxyl, and others, have all proven to be suitable. This approach may offer an interesting option when gold is needed anyway (e.g., in SPR experiments). Mixed thiol monolayers and microcontact printing of thiols are other promising approaches to obtain patterned substrates and arrays. Another approach is to use silane chemistry on silicon/silicon dioxide or glass. Many silanes have proven to produce organic films suitable as grafting platforms.

Acknowledgment. We thank the Swedish Research Council (VR) and the Swedish Foundation for Strategic Research (SSF) for financial support.

References and Notes

(1) Löfås, S.; Johnsson, B. *J. Chem. Soc., Chem. Commun.* **1990**, 1526–1528.
(2) Muñoz, E. M.; Yu, H.; Hallock, J.; Edens, R. E.; Linhardt, R. J. *Anal. Biochem.* **2005**, *343*, 176–178.
(3) Yu, H.; Muñoz, E. M.; Edens, R. E.; Linhardt, R. J. *Biochim. Biophys. Acta (BBA)—Gen. Subjects* **2005**, *1726*, 168–176.
(4) Webster, C. I.; Cooper, M. A.; Packman, L. C.; Williams, D. H.; Gray, J. C. *Nucleic Acids Res.* **2000**, *28*, 1618–1624.
(5) Mori, Y.; Nagaoka, S.; Takiuchi, H.; Kikuchi, T.; Noguchi, N.; Tanzawa, H.; Noishiki, Y. *Trans. Am. Soc. Artif. Intern. Organs* **1982**, *28*, 459–463.
(6) Desai, N. P.; Hubbell, J. A. *J. Biomed. Mater. Res.* **1991**, *25*, 829–843.
(7) Harris, J. M. *Poly(Ethylene Glycol) Chemistry: Biotechnical and Biomedical Applications*; Plenum Press: New York, 1992.
(8) Lee, J. H.; Jeong, B. J.; Lee, H. B. *J. Biomed. Mater. Res.* **1997**, *34*, 105–114.
(9) Zhang, M.; Desai, T.; Ferrari, M. *Biomaterials* **1998**, *19*, 953–960.
(10) Kenausis, G. L.; Vörös, J.; Elbert, D. L.; Huang, N.; Hofer, R.; Ruiz-Taylor, L.; Textor, M.; Hubbell, J. A.; Spencer, N. D. *J. Phys. Chem. B* **2000**, *104*, 3298–3309.
(11) Huang, N.-P.; Michel, R.; Vörös, J.; Textor, M.; Hofer, R.; Rossi, A.; Elbert, D. L.; Hubbell, J. A.; Spencer, N. D. *Langmuir* **2001**, *17*, 489–498.
(12) Hansson, K. M.; Tosatti, S.; Isaksson, J.; Wetterö, J.; Textor, M.; Lindahl, T. L.; Tengvall, P. *Biomaterials* **2005**, *26*, 861–872.
(13) Alcantar, N. A.; Aydil, E. S.; Israelachvili, J. N. *J. Biomed. Mater. Res.* **2000**, *51*, 343–351.
(14) Xu, D.; Yu, W. H.; Kang, E. T.; Neoh, K. G. *J. Colloid Interface Sci.* **2004**, *279*, 78–87.
(15) Ko, Y. G.; Kim, Y. H.; Park, K. D.; Lee, H. J.; Lee, W. K.; Park, H. D.; Kim, S. H.; Lee, G. S.; Ahn, D. J. *Biomaterials* **2001**, *22*, 2115–2123.
(16) Gabriel, S.; Dubruel, P.; Schacht, E.; Jonas, A. M.; Gilbert, B.; Jérôme, R.; Jérôme, C. *Angew. Chem., Int. Ed.* **2005**, *44*, 5505–5509.
(17) Fujimoto, K.; Inoue, H.; Ikada, Y. *J. Biomed. Mater. Res.* **1993**, *27*, 1559–1567.
(18) Uchida, E.; Uyama, Y.; Ikada, Y. *Langmuir* **1994**, *10*, 481–485.
(19) Noh, I.; Hubbell, J. A. *J. Polym. Sci., Part A: Polym. Chem.* **1997**, *35*, 3467–3482.
(20) Wang, P.; Tan, K. L.; Kang, E. T. *J. Biomater. Sci., Polym. Ed.* **2000**, *11*, 169–186.
(21) Cheo, S. H. Y.; Wang, P.; Tan, K. L.; Ho, C. C.; Kang, E. T. *J. Mater. Sci.: Mater. Med.* **2001**, *12*, 377–384.
(22) Wang, P.; Tan, K. L.; Kang, E. T.; Neoh, K. G. *J. Mater. Chem.* **2001**, 2951–2957.
(23) Zhang, F.; Kang, E. T.; Neoh, K. G.; Huang, W. *J. Biomater. Sci., Polym. Ed.* **2001**, *12*, 515–531.
(24) Zhang, F.; Kang, E. T.; Neoh, K. G.; Wang, P.; Tan, K. L. *Biomaterials* **2001**, *22*, 1541–1548.
(25) Piehler, J.; Brecht, A.; Valiokas, R.; Liedberg, B.; Gauglitz, G. *Biosens. Bioelectron.* **2000**, *15*, 473–481.
(26) Huang, N.-P.; Vörös, J.; De Paul, S. M.; Textor, M.; Spencer, N. D. *Langmuir* **2002**, *18*, 220–230.
(27) Masson, J.-F.; Battaglia, T. M.; Kim, Y.-C.; Prakash, A.; Beaudoin, S.; Booksh, K. S. *Talanta* **2004**, *64*, 716–725.
(28) Griesser, H. J.; Chatelier, R. C.; Gengenbach, T. R.; Vasic, Z. R.; Johnson, G.; Steele, J. G. In *Surface engineering: processes and applications*; Stafford, K. N., Smart, R. S. C., Sare, I., Subramanian, C., Eds.; Technomic Publishing AG: Basel, Switzerland, 1995; p 380.
(29) Suzuki, M.; Kishida, A.; Iwata, H.; Ikada, Y. *Macromolecules* **1986**, *19*, 1804–1808.
(30) Kang, E. T.; Tan, K. L.; Kato, K.; Uyama, Y.; Ikada, Y. *Macromolecules* **1996**, *29*, 6872–6879.
(31) Nho, Y. C.; Kwon, O. H. *Radiat. Phys. Chem.* **2003**, *66*, 299–307.
(32) Lee, J. H.; Kopecek, J.; Andrade, J. D. *J. Biomed. Mater. Res.* **1989**, *23*, 351–368.
(33) Jeon, S. I.; Lee, J. H.; Andrade, J. D.; Gennes, P. G. d. *J. Colloid Interface Sci.* **1991**, *142*, 149–158.
(34) Ostuni, E.; Chapman, R. G.; Liang, M. N.; Meluleni, G.; Pier, G.; Ingber, D. E.; Whitesides, G. M. *Langmuir* **2001**, *17*, 6336–6343.

CDV

(35) Unsworth, L. D.; Sheardown, H.; Brash, J. L. *Langmuir* **2005**, *21*, 1036−1041.
(36) Prime, K. L.; Whitesides, G. M. *Science* **1991**, *252*, 1164−1167.
(37) Prime, K. L.; Whitesides, G. M. *J. Am. Chem. Soc.* **1993**, *115*, 10714−10721.
(38) Benesch, J.; Svedhem, S.; Svensson, S. C. T.; Valiokas, R.; Liedberg, B.; Tengvall, P. *J. Biomater. Sci., Polym. Ed.* **2001**, *12*, 581−597.
(39) Higuchi, A.; Sugiyama, K.; Yoon, B. O.; Sakurai, M.; Hara, M.; Sumita, M.; Sugawara, S.-i.; Shirai, T. *Biomaterials* **2003**, *24*, 3235−3245.
(40) Tosatti, S.; Paul, S. M. D.; Askendal, A.; VandeVondele, S.; Hubbell, J. A.; Tengvall, P.; Textor, M. *Biomaterials* **2003**, *24*, 4949−4958.
(41) Lee, S.; Vörös, J. *Langmuir* **2005**, *21*, 11957−11962.
(42) Dordi, B.; Schönherr, H.; Vancso, G. J. *Langmuir* **2003**, *19*, 5780−5786.
(43) Biacore. *Sensor surface handbook*; Uppsala, Sweden, 2003.
(44) Larsson, O.; Öhman, O. *Micro Struct. Bull.* **1997**, *5*, 3.

BM060685G